Listening to the Sun: a Radio Telescope analysis of Solar Temperature

Diego Aguirre
Cornell University
(Dated 23 February, 2024)

A 12 GHZ Low Noise Block mounted to an 18" satellite dish can be aimed at the sun to measure the output power of the radio waves emitted. The noise temperature of LNB can be computed through calibration, allowing a rough estimate of the sun's temp to be obtained. Additional refinement by considering the solid angles involved yielded a value of 5183K ± 692K.

I. Introduction

All forms of matter emit some form of electromagnetic radiation. Leaning upon *Radio Astronomy* by John Kraus [1], we observe that by measuring the intensity of some incident radiation and then applying the Rayleigh-Jeans law, one can determine the temperature of the emitter.

For our purposes, we reference Kerry Smiths and Chuck Forster's *Itty Bitty Telescope* [2] to construct a 12 GHZ radio telescope. By assuming the interference in the sky to be minimal, we are able to take our initial measurement by aiming our telescope at the sun. In the lab we calibrate our apparatus by measuring a known source and varying attenuation. This yields a calibration curve - enabling us to convert our initial reading to a temperature value.

However, the sun is over 90 million miles away from earth. As a result, its solid angle is a mere fraction of our telescope's angle of radiation acceptance. To account for this, we first reference Young and Freedman to find the resolving power of our dish. We then reference Kraus' *Radio Astronomy* [1] once more to derive an expression that yields a refined value for the Sun's temperature.

II. Theory

By the *Rayleigh Jean Law* [3], we see: $T \propto P$ where T represents the source temperature, and P is the power reading. Following Hagen [3], we assert that the meter's power output is proportional to the intensity of the incident radiation plus the device's internal noise temp, and thus LNB generates intrinsic noise proportionally to the source temperature.

Equation 1 relates our reading D_1 to the Source Temp T, Room Temp T_1, and Noise Temp T_0 . a and b are both constants from our calibration process, in which we use a known temperature source to find T_0.

$$D_1 = a + b\,log[\frac{(T + T_0)}{(T_1 + T_0)}] \qquad (1)$$

Following *Young & Freedman* [4] and applying the *Rayleigh-Criterion* [4], we compute the solid angle of radiation acceptance for our dish. Observing that it is a mere fraction of the sun's solid angle [1], we refine our value through Equation 2:

$$T = \frac{(T_{sun} \times \Omega_{sun}) + (T_{sky} \times (\Omega_{ant} - \Omega_{sun}))}{\Omega_{ant}} \qquad (2)$$

where T_{sun} is the adjusted temperature value, T_{sky} is the cosmic background temperature, Ω_{sun} and Ω_{ant} are the solid angles of the Sun and Antenna respectively.

III. Apparatus

FIG. 1 overviews the components and their positions while measuring the sun and sky. The antenna of our radio telescope is a 18" satellite TV dish. Mounted to its arm is a 12 GHZ LNB. The LNB reads reflected signals off the dish's feed point and propagates them to Accutrac 22, which outputs a power.

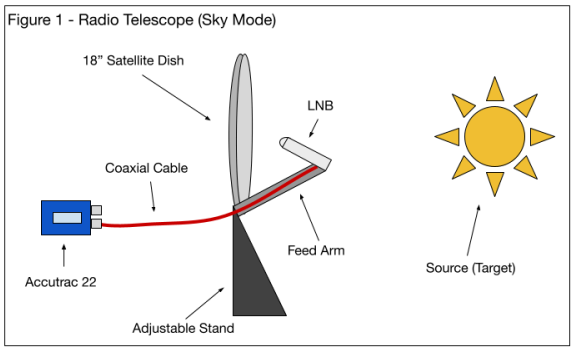

FIG. 1. The LNB is mounted to the dish via a feed arm, ensuring that the feedhorn is in alignment with the dish's feedpoint. The LNB then lowers the frequency of this signal with minimal loss, before transmitting it via coaxial cable to the Accutrac 22.

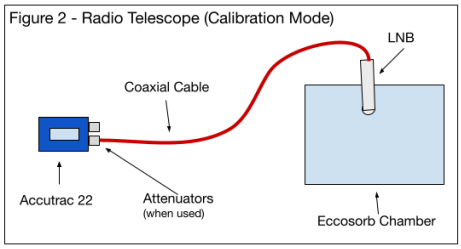

FIG. 2. The LNB measures the interior of the eccosorb chamber through its feedhorn. FAMP-HR (± 0.5 DB) and FAMP (±1 DB) attenuators are connected in between the LNB and Accutrac to plot the calibration curve.

FIG. 2 overviews the components and their positions during the calibration. The LNB is dismounted and placed within an eccosorb lined chamber. When used, attenuators are attached in series to the coaxial cable in between the LNB and Accutrac 22.

IV. Experiment

In order to accurately calculate the Sun's temperature, we began by calibrating our radio telescope at room temperature in the lab. The LNB was detached from the disk and inserted into an eccosorb lined container. Attenuation was varied from 0db to 16db by connecting attenuators in series with the Accutrac 22. This process was performed twice, first with FAMP and then with FAMP-HR attenuators; each yielded its own curve*. Additionally, 21 values were recorded with no attenuation and RSS was used to determine the uncertainty of the calibration setup.

To determine the combined uncertainty of our radio telescope, the apparatus was positioned atop the fourth floor balcony of PSB on a perfectly clear day. The dish was aimed at the blank sky, and 50 measurements were recorded. The standard deviation of this sample was denoted to be the Type A uncertainty of our radio telescope. The combined uncertainty was then computed using the RSS method.

Figure 3 - Distribution of Blank Sky Power Readings

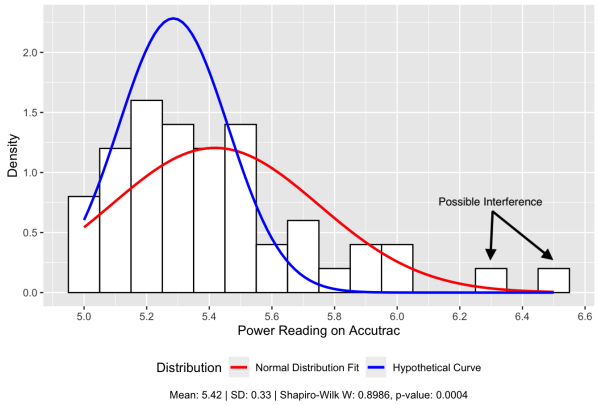

FIG. 3. The densities of different values recorded for the blank sky are shown. Discrepancy in tail behavior is logical due to cosmic background noise. A Shapiro test yields a p-value of 0.0004 indicating a poor normal fit.

Figure 4 - FAMP Attenuators vs Accutrac 22 Power Reading

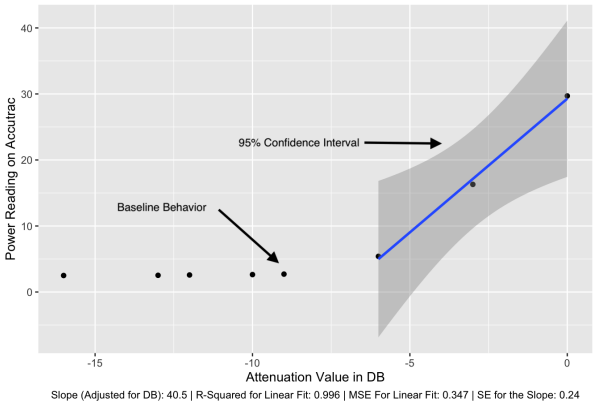

FIG. 4. Varying amounts of attenuation achieved using FAMP Attenuators and their corresponding power outputs. A linear regression on the lowest 3 attenuation values yields a slope of 40.5 with a standard error of 0.24.The mean squared of 0.347 suggests a strong linear fit.

The intrinsic noise was measured twice using liquid nitrogen and the sky as the known temperatures. Liquid nitrogen was poured into the eccosorb chamber and measurements were taken with no attenuation. For the sky, values from the PSB Patio were used. Denoting the means of these readings as D_2, using appropriate calibration constants and T values, two distinct values were computed.

To measure D_1, the apparatus was positioned outside Bailey Hall on a perfectly clear day. The dish was aimed at the sun and 5 values were recorded at 30 second intervals. Their mean was recorded as D_1.

Additionally, for a qualitative proof of concept, a 42 degree horizontal scan of the sky was taken on the PSB Patio on a clear day. This yielded the diffraction pattern for a satellite.

V. Results

The central result of this experiment were two values for the temperature of the sun. By calibrating our radio telescope and then aiming our apparatus at the sun on a clear sky, we obtained an approximate value. This initial estimate was refined by incorporating solid angle measurements into our calculations.

FIG. 3 displays a histogram of the Accutrac 22 readings when the radio telescope was aimed at the blank sky on a sunny day. We observe significant tail behavior on the upper end; which could be attributed to interference from higher intensity sources such as satellites. Minimal tail end behavior was observed on the lower end. The intrinsic cosmic background noise helps account for this floor. The red curve is a Normal Distribution Fit, and the corresponding Shapiro-Wilk test yields a p-value of 0.0004, indicating a poor normal fit. The blue curve represents a hypothetical fit that only considers meter values in [5.0, 5.6]; its p-value of 0.038 is an improvement, but still suggests that the data does not follow a normal distribution.

Figures 4 and 5 display the calibration curves that were recorded using FAMP and FAMP-HR attenuators respectively. The x-axis has been left in DB to make the plot easier to visualize, but the slope was computed with the aid of Equation 3, where P_{out} is the resultant power, P_{in} is the input power, and N is the attenuation in DB:

$$P_{out} = P_{in} \times 10^{\frac{-N}{10}} \qquad (3)$$

Due to the flatline behavior observed from 9db and up, only the lowest 3 attenuation values were considered during the linear fit. The FAMP-HR attenuators yielded a slope of 39.4 with a standard error of 0.19; FAMP attenuators yielded a slope of 40.5 and standard error of 0.24. The larger reported error for the FAMP curve is logical, given how their uncertainty is ±1 DB opposed to the ±0.5 DB of the FAMP-HR attenuators.

Two noise temperatures were computed. Using liquid nitrogen as the known source, 5 D_2 values were recorded in the lab with a mean of 23.54 and standard deviation of 0.054. The uncertainty in this measurement is 0.08 and was computed using RSS with Type A = 0.062 (computed using 21 measurements in the eccosorb chamber with no attenuation) and Type B = 0.05 (Accutrac 22). Using appropriate calibration constants, setting T to 77K and using Equation 1; T_0 was computed to be 412.97K ± 11.05K. Using the sky as the known source, the data taken from the PSB Patio, and setting T to 3k, a second noise temperature of 88.17K ± 2.52K was derived. The uncertainties in both of these values were computed using Monte Carlo simulations, both with n = 10,000.

The sun temperature was derived by first using Equation 1 and then adjusting the value for Solid Angle's through Equation 2 . Five D values were recorded at Bailey, with a mean of 9.32 and standard deviation of 0.15. The uncertainty in the measurement is ±0.33, and was computed using RSS with Type A = 0.33 (50 sky readings), and Type B = 0.05 (Accutrac 22). Using our sky-based Noise Temperature, an un-adjusted temperature of 26.4K ± 2.95K was derived. Applying Equation 2, a value of 5183K ± 689.6K was computed. Conversely, the liquid nitrogen based Noise Temperature yielded an un-adjusted temperature of -200.02K ± 8.92K and adjusted value of -42,052K ± 3324K.

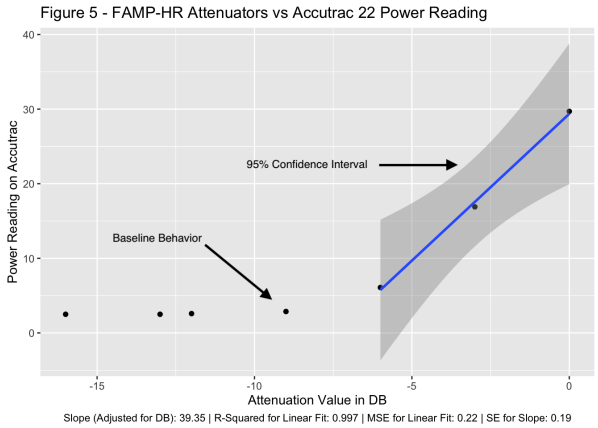

FIG. 5. Varying amounts of attenuation achieved using FAMP-HR Attenuators and their corresponding power outputs. A linear regression on the lowest 3 attenuation values yields a slope of 39.35 with a standard error of 0.19.The mean squared error of 0.22 suggests a strong linear fit.

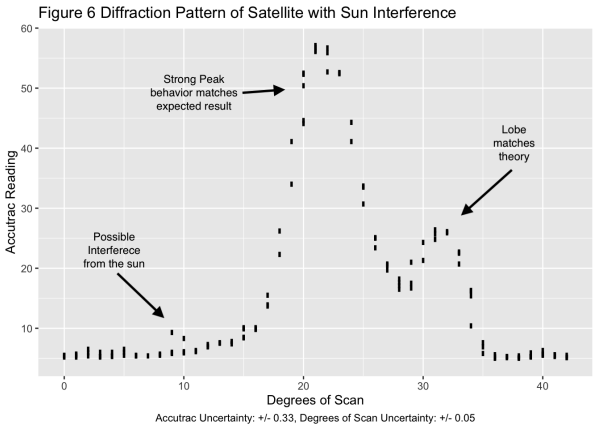

FIG. 6. Scatterplot shows the observed diffraction pattern, with numerous samples taken at each degree value. The Accutrac Uncertainty is graphically represented as the height of each bar, and the Degree Uncertainty is represented through the width.

The uncertainties in the unadjusted values were computed using Monte Carlo simulations, both with n = 10,000. Determining the uncertainty in the solid angle adjustment was cumbersome as our satellite dish was not a perfect sphere. Instead, a Monte-Carlo Simulation with n = 10,000 was run for following system of equations:

Equation #1 (solving for T_0)

Equation #1 (solving for T)

Equation #2 (solving for T_{sun})

Rayleigh Criterion: $Sin(\theta) = \frac{1.22\lambda}{d}$ [4]

Antiderivative of Solid Angle: $\Omega_{ant} = \pi\theta^2$

Where θ is the resolving power of the dish, λ is the wavelength of incident radiation, *d* is the diameter of the dish,and Ω_{ant} is the solid angle of the dish. For *d* in the Rayleigh Criterion [4], the average of the height and width of the dish were used, and its uncertainty was set to half of the difference between the two values.

FIG. 6 displays the Diffraction Pattern of the Satellite. The general shape resembles what was expected, but is asymmetric. Possible interference from the sun is observed at 10 degrees, as the sun was directly above where the dish was aimed[1] at this point.

VI. Conclusion

Using our two slightly different approaches, our methodology yields two distinct values for the sun's temperature. With the exception of the vastly differing noise temperatures, the majority of our results agreed with the expected outcomes. In both attenuation curves, the expected flatline behavior was observed; and the relationship between attenuation and resultant power yielded a strong linear fit. Additionally, with the exception of the missing lobe; the diffraction pattern outlined in FIG. 6 shows qualitative resemblance to the expected result.

We computed two values for the temperature of the sun: 5183K ± 689.6K using a noise temperature of 88.17K ± 2.52K, and -42,052.72K ± 3324.5K using a noise temperature of 412.97K ± 11.05K. The methods behind each noise temperature were identical with the exception of the known source, and the magnitude of the latter can be attributed to the D_2 reading of the Liquid Nitrogen. For both final temperatures, sensitivity analysis showed D_2 as having the second highest sensitivity behind the diameter of the dish.

As such, further experimentation is warranted to assess the validity of the noise temperature measurement systems. Additionally, a more meticulous treatment of this experiment should consider deriving a more precise system to measure the solid angle of the satellite dish. These measures would mitigate uncertainty, seeking to increase the validity of our experiment.

1

[1] *Radio Astronomy*, John D Kraus (McGraw Hill, New York, 1996)
[2] *Itty Bitty Telescope Notes*, Tom Crowley & Kerry Smith
[3] *Radio Frequency Electronics*, John B Hagen (Cambridge, Cambridge, 1999)
[4] *University Physics*, H.D. Young & R.H. Freedman (Pearson, San Francisco, 2008)